Optics Communications 282 (2009) 4537–4542

Contents lists available at ScienceDirect

Optics Communications

journal homepage: www.elsevier.com/locate/optcom

Optical studies of two dimensional gratings in fused silica, GE 124, and Foturan™ glasses fabricated using femtosecond laser pulses

K.C. Vishnubhatla [a], S. Venugopal Rao [b,*], R. Sai Santosh Kumar [a], Maurizio Ferrari [c], D. Narayana Rao [a,*]

[a] School of Physics, University of Hyderabad, Hyderabad 500046, India
[b] Advanced Centre of Research in High Energy Materials (ACRHEM), School of Physics, University of Hyderabad, Hyderabad 500046, India
[c] 1CNR-IFN, CSMFO Laboratory, via alla Cascata 56/c, Povo, 38050 Trento, Italy

ARTICLE INFO

Article history:
Received 15 April 2009
Received in revised form 22 August 2009
Accepted 22 August 2009

Keywords:
Femtosecond laser direct writing
Fused silica
GE 124
Foturan
Gratings

ABSTRACT

Herein we present results on the femtosecond laser direct writing and optical characterization studies of two dimensional gratings in fused silica, GE 124, and Foturan™ glasses. Varieties of structures were achieved with varying input energy and spatial orientation of the samples. Various characterization techniques including fluorescence spectroscopy, micro-Raman spectroscopy, and laser confocal microscopy were employed to analyze the structural and physical modifications at the focal volume resulting in change of refractive index. Diffraction efficiencies of ~9–12% were observed from the grating structures. A broad-band emission was observed in the laser-modified region of the Foturan glass. The obtained results are analyzed in the light of recent work in similar glasses and exploring the applications of such structures in the fields of photonics.

1. Introduction

The ability to pattern materials in pre-determined manner and in three dimensions is appealing for several emerging technologies like bio-photonics and microfluidics/optofluidics [1–4]. Femtosecond (fs) direct writing is capable of creating three dimensional micro- and nano-structures deep inside bulk of a dielectric or polymeric material [5–10]. This technique offers exciting prospects for miniaturization and integration of highly functional photonic and microfluidic devices directly inside transparent dielectrics and polymers alike [11–17]. In contrast to standard methods such as physical-vapor deposition or ion exchange, a direct write approach is not constrained to the surface and yields truly three-dimensional structures. The ultrafast interaction does not require specially prepared or photosensitive materials making this technique less material-dependent in comparison to others. Several photonic and microfluidic structures/devices have been demonstrated recently ratifying the enormous potential of this technique. Some of the diverse structures/devices produced using this method are (a) waveguides in laser crystals such as Ti:Sapphire and Nd:YAG ceramics [18–20]; (b) variety of microfluidic structures in Foturan™ leading to lab-on-a-chip devices [21–27]; (c) waveguides in periodically poled lithium niobate (PPLN) [28]; (e) waveguide lasers in the telecom band [29,30]; (f) micro- and nano-structures and channels [31–38]; (g) photonic crystal structures, etc. A comprehensive review on the physics and applications of this technique is presented in Refs. [7–12]. Some of the fascinating applications demonstrated utilizing fs direct writing technique include: (i) exclusive repair of expensive X-ray masks; (ii) demonstration of nano-aquarium for microscopic observation of aquatic microorganisms; (iii) joining/welding two similar and dissimilar glasses [39], and (iv) laser calligraphy [40]. However, there have been modest efforts towards studies on two/three dimensional grating structures in glasses, which are one of the basic building blocks in photonics.

Here, we present some of our results on the direct writing and characterization of micro-structures/gratings in silicate (GE 124 and fused silica) and Foturan™ glasses. Micro-structures with different sizes and shapes were fabricated with varying input energy and orientation of the sample. Various characterization techniques including fluorescence spectroscopy, micro-Raman spectroscopy, and confocal microscopy were employed to analyze the structural and physical modifications. Interestingly, fluorescence was observed from the laser exposed regions of Foturan™. Applications of the structures created in these glasses are also discussed.

2. Experimental

All the samples were typically cut to a dimension of 1 cm × 2 cm for ease of use and all the six faces were optically polished.

* Corresponding authors. Fax: +91 40 23012800 (S.V. Rao).
E-mail addresses: svrsp@uohyd.ernet.in (S.V. Rao), dnrsp@uohyd.ernet.in (D.N. Rao).

0030-4018/$ - see front matter © 2009 Elsevier B.V. All rights reserved.
doi:10.1016/j.optcom.2009.08.041

Samples were cleaned first using acetone and then with methanol to ensure that the surface is devoid of any stains and dust. The cleaned samples were placed on computer controlled XYZ nanopositioner (NanoDirect Stages NTS 25, Discovery Tech International). The quality of the fabricated structures depended critically on the quality of the focused spot and on movement of the sample placed on XYZ stage. Any aberration in the optics or stage movement affected the shape and size of the structures considerably. Details of the experimental set up is reported elsewhere [41]. Typically, near-transform limited (~100 fs) pulses from an amplifier were employed for the direct writing at of 800 nm with 1 kHz repetition rate. Neutral density filters were used to control intensity of the input pulses. The beam was steered such that it focused downwards onto the sample after passing through the microscope objective (40X, 0.65 NA). The input beam diameter and the physical aperture of the objective were ~6 mm. Typical writing speeds of 250–500 μm/s were used. In the case of Foturan® the gratings were written with two different stages, the first was a translation stage with 2 μm resolution (Holmarc, India) and second was a stage with 20-nm resolution capability (NanoDirect Stages NTS 25, Discovery Tech International). Typical energies estimated before the sample were <30 μJ. The polarization of laser beam was perpendicular to the sample translation direction.

The procedure followed for inscribing and characterizing the gratings is as follows. Initially simple straight line structures were inscribed in the samples. Each line corresponded to a specific set of parameters (e.g. sample translation speed, intensity of the fs pulses, and size of aperture before the microscope objective). Later, these structures were imaged using scanning confocal microscope (Lieca) in both transmission and reflection modes. The widths of structures were determined in transmission mode. In the reflection mode several snapshots of the structures were taken along the depth at definite intervals (typically the step size along the *z*-axis was chosen to be ~1 μm). Each snapshot corresponded to a particular depth and all these snapshots were collated to obtain a 3-D (cross-sectional, depth profile) view of the written structures. The qualities of fabricated structures depend on several factors such as wavelength, repetition rate, focal conditions, pulse duration, pulse energy, writing speeds, and wave-front tilt [10,33,37]. On the basis of these preliminary tests an optimum configuration was determined to write gratings or waveguides in different glasses. We have investigated 2-D grating structures in GE 124, fused silica, and Foturan™ glasses.

3. Results and discussion

For fabrication of large-area gratings, the samples were translated perpendicular to the written line by a definite distance and then another line, parallel to the previous one, was inscribed. Following this approach a set of about 100 parallel lines (separated by 4–5 μm) were inscribed creating in the sample periodic alternating regions exposed and un-exposed to fs laser irradiation. Figs. 1a–d and 2a shows the gratings inscribed in fused silica and GE 124 glass, respectively. GE 124 is a type of fused quartz glass. The main differences are that fused quartz has a much lower OH content and fused silica transmits better in the UV. Both are highly pure, have high chemical resistance, good thermal shock resistance, and low thermal expansion coefficient. For achieving the 2-D gratings sets of such parallel lines crossing each other at 90° [Fig. 1b], 120° [Fig. 1c], and 60° [Fig. 1d] were written. These periodic regions of modified and unmodified RI act as a grating. This demonstrates the ability of the laser direct writing (LDW) process to create any structure, potentially leading to the fabrication of 2-D and 3-D photonic crystals. These structures inscribed in glasses were utilized to estimate the change in refractive index due to fs laser modification through the grating efficiency measurements. A He–Ne laser (633 nm) beam was incident perpendicular to the plane of the gratings and, the diffraction patterns were recorded on a screen placed 20 cm away from the sample. Inset of figures demonstrates the images of diffraction pattern. The power of the different laser spots corresponding to the different orders of diffraction were measured using a power meter (Ophir, PD300-3 W-V1). The grating diffraction efficiency, defined as the fraction of power diffracted into the first order compared to the input power, was calculated to be 9.5 ± 0.95% for the first order in fused silica and 11 ± 1.1% in GE 124 glass. The error bars indicate the inaccuracies in power measurements, positioning of the grating, and other scattering mechanisms. The change in the refractive index (Δn), assuming a pure refractive index change, was estimated to be of the order of 10^{-3} using

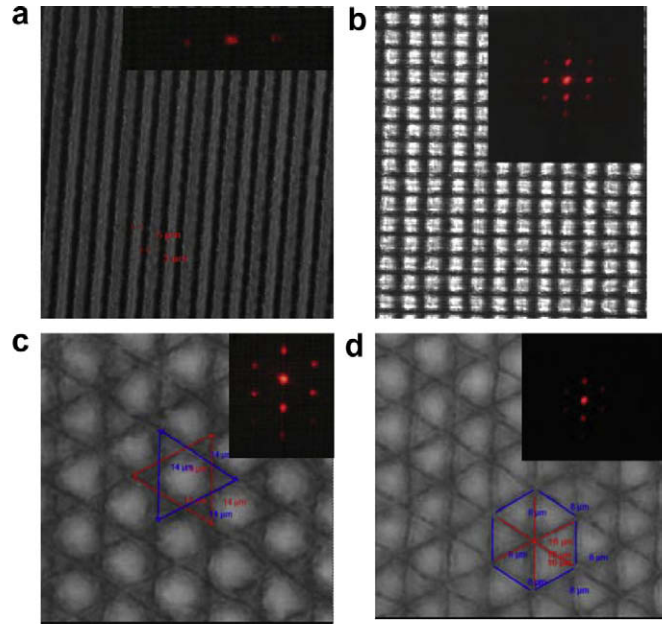

Fig. 1. (a)–(d) Confocal images of various two dimensional gratings written in fused silica glass. Inset shows the optical diffraction pictures.

$$\Delta n = \lambda \cos\theta \tanh^{-1}(\sqrt{\eta})/(\pi d) \quad (1)$$

where η is the first order diffraction efficiency (defined as ratio of input power to the power diffracted into first order), λ being the wavelength (632 nm), $\theta = 0°$ (normal incidence), d is the grating depth or thickness.

The Δn values obtained for the gratings are summarized in Table 1. Diffraction efficiency measurements for the gratings fabricated in Foturan™ glass were performed using the procedure described above. Several groups have successfully demonstrated waveguides, voids, channels, modulators, Bragg gratings, etc. [42–52] using direct writing in fused silica. Liu et al. [50] reported fabrication of gratings in fused silica with a diffraction efficiency of 7.9% for the first order which is lower than the value obtained in the present study. However, they also achieved 25% efficiency with multi-layer gratings. The RI change observed in their case, similar to ours, was ~10^{-3}. Ihlemann et al. [52] used F_2 laser and fabricated gratings with first order diffraction efficiency of 8% was measured. We believe that the efficiency can be improved further through use of multi-layer technique [50].

In the case of fused silica and GE 124 there is possibility of void formation since the input energies used for inscribing the gratings are sufficient to create voids [53–61]. However, our Raman and confocal studies did not provide any conclusive evidence for the void

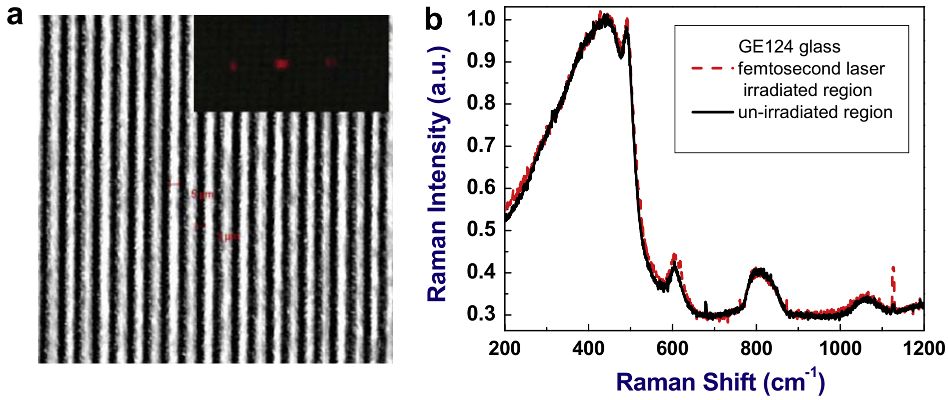

Fig. 2. (a) Optical microscope image of the GE 124 glass grating with diffracted laser pattern shown in the inset. (b) micro-Raman spectra obtained from irradiated (solid, black) and non-irradiated regions (dashed, red). (For interpretation of the references to color in this figure legend, the reader is referred to the web version of this article.)

Table 1
Summary of dimensions of the structures achieved in various samples along with the efficiencies of diffraction and the corresponding RI change measured. Incident energies were estimated after accounting for the microscope objective and other transmission losses from the experimental set up.

Sample	Incident energy (μJ)	Dimension of structure (μm)	Grating period (μm)	Efficiency (%)	Δn ($\times 10^{-3}$)
Fused silica	<30	4	4	9.5 ± 0.95	~2.1
GE 124	<35	5	5	11 ± 1.1	~2.0
Foturan	<35	4	4	10 ± 1.0	~2.2

formation. It is well established in silicate based glasses that voids are generally formed when high NA (>0.5) focusing conditions are employed. Void formation depends critically on the numerical aperture of the focusing lens used. The threshold for void formation increases with increase in depth at which it is created. After critical analyses of our experimental data, we noticed that there are several important points to be distinguished in our case: (a) the grating writing speed was 500 μm/s demonstrating that a single pulse is incident in a region of <0.5 μm of the sample. (b) No dispersion compensation optics was introduced in our experiment suggesting that the pulses could have broadened at the focus. Assuming the spot size at focus to be ~1.5 μm there is likelihood that, at best, three pulses are incident on the same area. With 0.65 NA and 25 μJ input energy, we do not rule out the formation of voids in our case. The size of the voids (or void like structures) created are estimated to be <1.0 μm in this case. (c) We did not employ any pulse shaping in our experiment. The area of modified regions in our samples were ~4–5 μm (width) × 40–60 μm (depth) [and elliptical in shape] implying that the void(s) contribution to the modified regions is insignificant. Song et al. [53] reported void array formation, formed 200 μm below the surface, in fused silica glass with 50 μJ energy focused using 0.9 NA (100X) objective lens and 32 pulses. The size of the voids was few μm. It is evident that (i) the energies used were much higher than in our case (ii) NA was higher than in our case (iii) number of pulses used were also higher than in our case. (e) Hashimoto et al. [54] reported void recording in silica (synthetic quartz glass, VOISIL) using energies of few hundred nano Joules with single pulse and 1.35 NA optics. They fabricated gratings using these voids and found that the diffraction efficiency increased with increase in order. We did not observe any such anomaly clearly suggesting the minimal role of voids in our case. However, we do not rule out the possibility that the gratings fabricated in fused silica and GE could contain void like structures embedded within the smooth refractive index change region. Further detailed studies are essential to arrive at tangible conclusions, which are in progress.

To examine the interaction of fs pulses with fused silica/GE 124 glass network we performed micro-Raman measurements in the fs laser-irradiated and un-irradiated regions. The samples were excited with 514 nm and Fig. 2b shows the micro-Raman spectra obtained in two regions of the GE 124 sample. Solid curve (black) represents the spectrum obtained from the region un-exposed to fs pulses while the red (dashed) curve relates to the fs-irradiated region. In both cases, the typical Raman spectrum of silica glass is observed [62]. The bands at 430, 800, 1100, and 1190 cm^{-1} are assigned to the vibrations of silica network. The two sharp bands at 490 and 606 cm^{-1} are called D_1 and D_2 defect bands, respectively. They are related to symmetric breathing modes of regular 4- and 3- membered silica rings [63]. These defect bands are slightly more intense in the spectrum of the irradiated region than in the un-irradiated one, particularly the D_2 defect band. The fused silica structural network typically has predominantly large five- and sixfold ring structures. An increase in D_2 and D_1 peak intensity corresponds, therefore, to an increase in the relative number of three- and fourfold planar ring structures in the glass network. As a consequence, the overall bond angle distribution is reduced, thus leading to a densification of the glass [45,55].

Earlier reports [42–45] also suggest that the possible mechanism of RI change in fused silica glass to be breakage of bonds in the network leading to densification and hence increase in refractive index in laser-modified region. We expect similar behaviour in GE 124 glass network. The RI change achieved varied from 10^{-3} to 10^{-4} depending on the writing conditions. For further investigation we looked at the absorption spectra of the modified and pristine regions. Fig. 3 shows the transmission behaviour for all the glasses studied in this work. There is an evident change in transmission spectra of the irradiated regions in comparison to those un-irradiated and the effect is more important in the case of fused silica and GE 124 glasses. The decrease in transmittance of the written region could possibly be attributed to (a) absorption resulting from the defects created during the LDW process and/or (b) scattering losses resulting from the inscribed gratings. FTIR spectra were also recorded and the results indicated no changes before and after irradiation with fs pulses.

Foturan, a photosensitive glass, comprises lithium aluminosilicate glass doped with traces of silver and cerium. The cerium (Ce^{3+}) ion plays an important role as photosensitizer, which releases an electron to become Ce^{4+} with exposure to UV light. Some silver ions are reduced by the free electrons and silver atoms are created. However, in the case of fs laser irradiation, free electrons

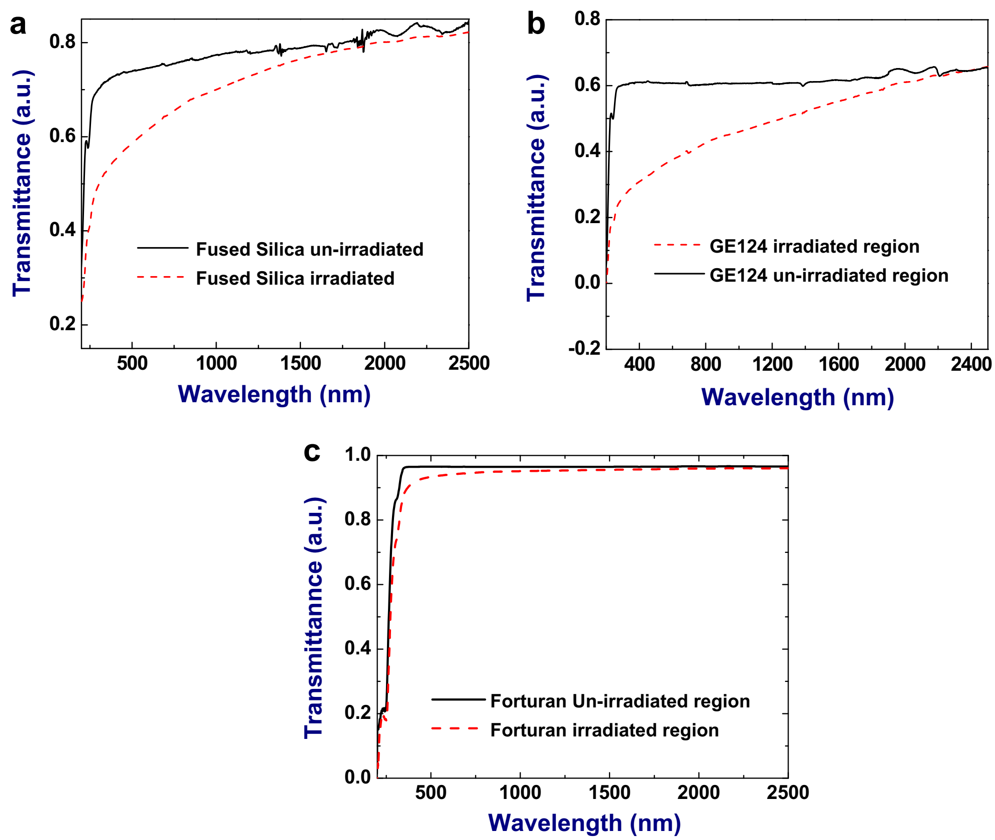

Fig. 3. Transmission spectra of the un-irradiated (solid, black) and fs-irradiated regions of the glass sample (dashed, Red) (a) fused silica, (b) GE 124 glass, and (c) Foturan®. (For interpretation of the references to colour in this figure legend, the reader is referred to the web version of this article.)

are generated by inter-band excitation due to multi-photon absorption for silver atom precipitation. Therefore, Ce^{3+} doping is not necessary for fs laser direct writing applications. Subsequent heat treatment assists the silver atoms diffusion and agglomeration to form nanoclusters near 500 °C followed by the crystalline phase of lithium metasilicate which then grows in the amorphous glass matrix in the vicinity of the silver nanoclusters, acting as nucleus, near 600 °C. Since the crystalline phase of lithium metasilicate has higher solubility in a dilute solution of HF acid than the glass matrix, it can be easily etched away leaving behind empty channels/voids. Midorikawa's group has reported results from their pioneering work of fs modification in Foturan™ for applications in lab-on-a-chip and microfluidics [21–27,64–67]. Different structures fabricated in Foturan glass using ultrashort pulses and ion beams include waveguides, micro-mechanical and micro-optical components, microfluidic dye lasers, and micro-channels, all integrated on a single chip leading to lab-on-a-chip device applications [65–75].

Micro-gratings were inscribed inside Foturan™ glass with different grating periods. Fig. 4 shows the confocal image of a typical grating in Foturan™. The change in refractive index was estimated to be 2.2×10^{-3} from the diffraction efficiency (~10% for the first order) measurements. The measurements were performed on the sample without annealing. Cheng et al. [23] reported gratings with a maximum efficiency of 1.4%. They utilized ~70 nJ, 140 fs pulses at 775 nm combined with a 50X (0.85 NA) microscope objective. They chose low intensity pulses to avoid optical breakdown for achieving higher spatial resolution. Bettiol et al. [75] used proton beam to inscribe gratings and obtained poor diffraction efficiency, measured at 473 nm.

The transmission spectrum collected from the modified region [Fig. 3c] shows a slight decrease in transmittance. This could be attributed to formation of color centres associated with Ag^{+}. Raman spectrum from the laser-irradiated region could not be obtained due to strong fluorescence covering the Raman bands. Confocal photoluminescence (PL) was obtained by exciting the sample with

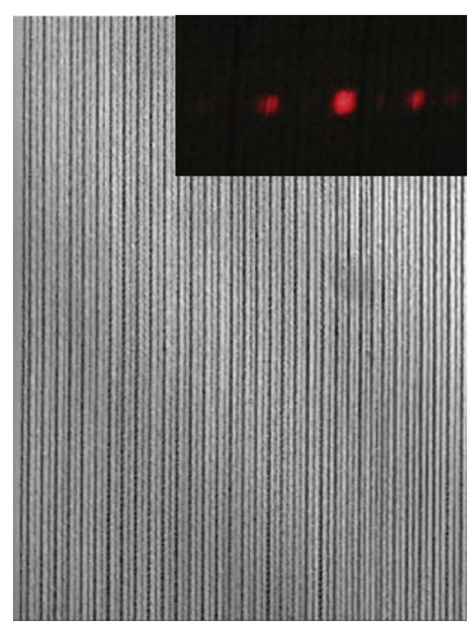

Fig. 4. Confocal image of a typical grating fabricated in Foturan glass. The structure separation and the structure width were ~4 µm. Inset shows the optical diffraction image.

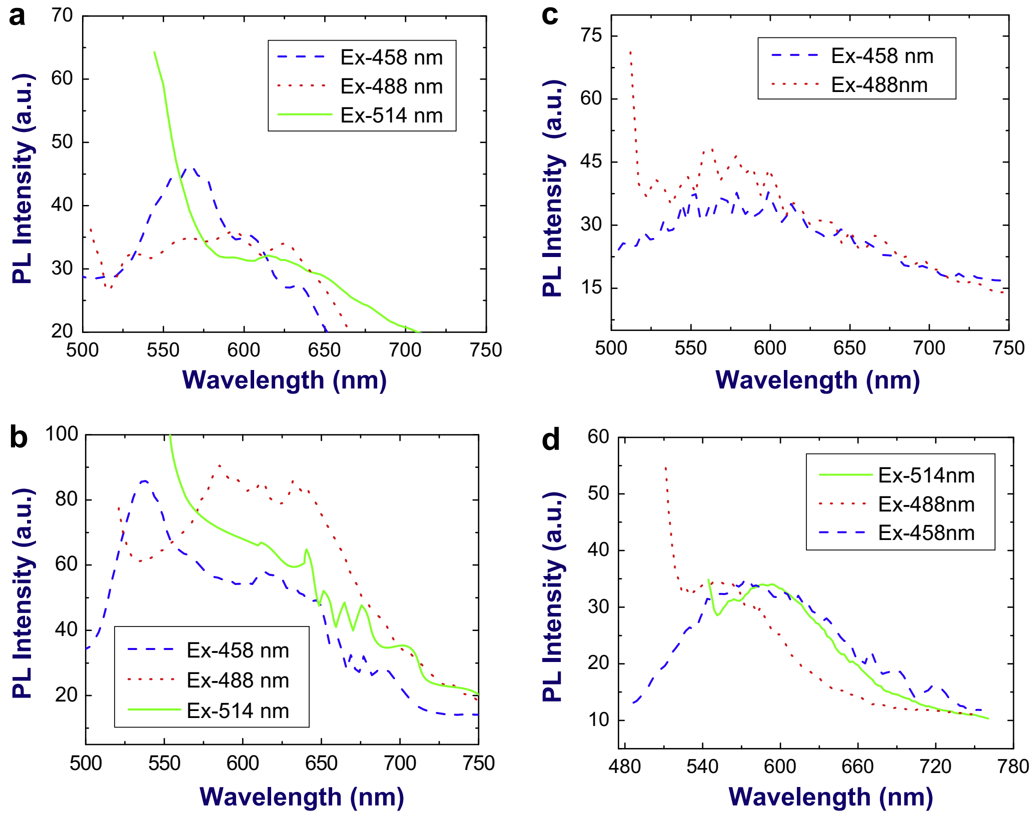

Fig. 5. Photoluminescence spectra of the fs laser-irradiated region in Foturan™. Solid (Green) line represents emission obtained by excitation at 514 nm, dashed (blue) line represents emission obtained by excitation at 458 nm while the blue line (dotted) was by excitation at 458 nm. (a) Data obtained for structures written with normal stage, immediately after exposure. (b) Data obtained after 3 months after exposure. (c) Data obtained for structures written with nano-stages, immediately after exposure and (d) after 3 months after exposure. (For interpretation of the references to colour in this figure legend, the reader is referred to the web version of this article.)

the 457, 488, and 514 nm lines of a cw Ar^+ laser. The confocal microscope was used in the XY-lambda mode. In this mode the microscope collected the photoluminescence from the region of interest in the sample over the range specified in intervals typically of 3 nm width. The region of interest in the sample was excited with laser light and the PL was collected for a specified time interval from the entire region of interest. PL in this band of wavelength was stored as intensity pattern. The collection window then moved to the next consecutive band of wavelength and the PL was recorded. This process was repeated until the entire specified range of wavelength was scanned by changing the collection window. Once the entire range was scanned the intensity patterns corresponding to the various wavelength intervals were integrated to obtain a plot of intensity versus wavelength. Only the region irradiated with fs laser showed clear photoluminescence band. The maximum of the emission band shifted with the excitation wavelength as shown in Fig. 5. Fig. 5a and b depicts the PL spectra in Foturan™ structures written with normal stage (Holmarc, India, 2 μm resolution) obtained immediately after writing and after 90 days, respectively. Fig. 5c and d presents the PL from structures written with a nanopositioner recorded immediately after writing and after 90 days, respectively. This data confirmed that the PL was not temporary/short-lived and sustained for long time.

Though this kind of photoluminescence was observed in Ag doped phosphate glasses [76], to our knowledge this is the first observation in Foturan glass. We expect the presence of color centres in the light modified regions contributing to the observed PL. However, it is well established that these color centres disappear during thermal annealing process implying that these fluorescing centres should be generated after the necessary etching steps have been executed for the creation of micro-channels in device fabrication. Since Foturan™ is proficiently used for microfluidic studies, the observation of PL is an important development and will find impending applications in lab-on-a-chip and sensor applications as a broad-band source. The ability to fabricate different microstructures in various glasses has implications in various fields of telecommunications and biotechnology. Integrating simple passive structures such as waveguides, gratings, couplers, splitters, etc. along with active devices such as laser sources, detectors will lead to photonic integrated circuits while integration of optical components and microfluidic components like channels, reservoirs, etc. will lead to optofluidic lab-on-a-chip devices capable of on-site diagnosis.

4. Conclusions

We have successfully fabricated micro-gratings in silicate and Foturan™ glasses using femtosecond direct writing. Refractive index change in these structures was estimated using optical diffraction technique and was found to be in the order of 10^{-3} sufficient for wave guiding applications. Several characterization techniques were used for insight into the fs interaction with the glass matrix. The ability to create such structures, both passive and active, has strong implications in the field of micro-photonic and microfluidic devices.

Acknowledgments

S. Venugopal Rao thanks the Department of Science of Technology, India for financial support through a SERC project SR/S2/LOP-

11/2005. D.N.R., M.F., R.S.S.K, and K.C.V. acknowledge the financial support from ITPAR project and CSIR, India. The authors acknowledge Dr. P.S.R. Prasad for assistance in acquiring the micro-Raman spectra. Dr. V. Nirmal Kumar, Dr. R. Ramponi, and Dr. R. Osellame are acknowledged for useful discussions.

References

[1] D.B. Weibel, W.R. DiLuzio, G.M. Whitesides, Nature 5 (2007) 209.
[2] C. Monat, P. Domachuk, B.J. Eggleton, Nat. Photonics 1 (2007) 106.
[3] J.A. Lewis, G.M. Gratson, Mater. Today 7 (7–8) (2004) 32.
[4] D.B. Chrisey, Science 289 (2000) 879.
[5] K.M. Davis, K. Miura, N. Sugimoto, K. Hirao, Opt. Lett. 21 (1996) 1729.
[6] C.B. Schaffer, A. Brodeur, J.F. Garcia, E. Mazur, Opt. Lett. 26 (2001) 93.
[7] J. Qiu, K. Miura, K. Hirao, J. Non-Cryst. Solids 354 (2008) 1100.
[8] S. Juodkazis, V. Mizeikis, S. Matsuo, K. Ueno, H. Misawa, Bull. Chem. Soc. Jpn. 81 (4) (2008) 411.
[9] G. Della Valle, R. Osellame, P. Laporta, J. Opt. A: Pure Appl. Opt. 11 (2009) 013001.
[10] R.R. Gattass, E. Mazur, Nat. Photonics 2 (2008) 219.
[11] K. Itoh, W. Watanabe, S. Nolte, C.B. Schafer, MRS Bull. 31 (2006) 620.
[12] M. Kohtoku, T. Kominato, Y. Nasu, T. Shibata, NTT Tech. Rev. 3(7) (2005).
[13] J. Qiu, K. Kojima, K. Miura, T. Mitsuyu, K. Hirao, Opt. Lett. 24 (1999) 786.
[14] E.N. Glezer, E. Mazur, Appl. Phys. Lett. 71 (2007) 882.
[15] Y. Shimotsuma, K. Hirao, J. Qiu, K. Miura, J. Non-Cryst. Solids 352 (2006) 646.
[16] K. Sugioka, Y. Hanada, K. Midorikawa, Prog. Electromag. Res. Lett. 1 (2008) 181.
[17] M. Ams, G.D. Marshall, P. Dekker, M. Dubov, V.K. Mezentsev, I. Bennion, M.J. Withford, IEEE J. Sel. Top. Quantum Electron. 14 (5) (2008) 1370.
[18] V. Apostolopoulos, L. Laversenne, T. Colomb, C. Depeursinge, R.P. Slathé, M. Pollnau, R. Osellame, G. Cerullo, P. Laporta, Appl. Phys. Lett. 85 (2004) 1122.
[19] G.A. Torchia, P.F. Meilán, A. Rodenas, D. Jaque, C. Mendez, L. Roso, Opt. Express 15 (2007) 13266.
[20] J. Lamela, A. Rodenas, D. Jaque, F. Jaque, Opt. Express 15 (2007) 3285.
[21] K. Sugioka, M. Masuda, T. Hongo, Y. Cheng, K. Shihoyama, K. Midorikawa, Appl. Phys. A 79 (2004) 815.
[22] Y. Cheng, K. Sugioka, K. Midorikawa, Opt. Lett. 29 (2004) 2007.
[23] Y. Cheng, K. Sugioka, M. Masuda, K. Shihoyama, K. Toyoda, K. Midorikawa, Opt. Express 11 (2003) 1809.
[24] M. Masuda, K. Sugioka, Y. Cheng, N. Aoki, M. Kawachi, K. Shihoyama, K. Toyoda, H. Helvajian, K. Midorikawa, Appl. Phys. A 76 (2003) 857.
[25] Y. Cheng, K. Sugioka, K. Midorikawa, M. Masuda, K. Toyoda, M. Kawachi, K. Shihoyama, Opt. Lett. 28 (2003) 1144.
[26] K. Sugioka, Y. Hanada, K. Midorikawa, Appl. Surf. Sci. 253 (2007) 6595.
[27] Y. Cheng, Z. Xu, K. Sugioka, K. Midorikawa, Proc. SPIE 6400 (2006) 64001.
[28] R.R. Thomson, S. Campbell, I.J. Blewett, A.K. Kar, D.T. Reid, Appl. Phys. Lett. 88 (2006) 111109.
[29] S. Taccheo, G. Della Valle, R. Osellame, G. Cerullo, N. Chiodo, P. Laporta, O. Svelto, A. Killi, U. Morgner, M. Lederer, D. Kopf, Opt. Lett. 29 (2004) 2626.
[30] R. Osellame, N. Chiodo, G. Della Valle, G. Cerullo, R. Ramponi, P. Laporta, A. Killi, U. Morgner, O. Svelto, IEEE J. Sel. Top. Quantum Electron. 12 (2006) 227.
[31] V. Maselli, R. Osellame, G. Cerullo, R. Ramponi, P. Laporta, L. Magagnin, P.L. Cavllotti, Appl. Phys. Lett. 88 (2006) 191107.
[32] C. Hnatovsky, R.S. Taylor, P.P. Rajeev, E. Simova, V.R. Bhardwaj, D.M. Rayner, P.B. Corkum, Appl. Phys. Lett. 87 (2005) 014104.
[33] V.R. Bhardwaj, E. Simova, P.P. Rajeev, C. Hnatovsky, R.S. Taylor, D.M. Rayner, P.B. Corkum, Phys. Rev. Lett. 96 (2006) 057404.
[34] Y. Shimotsuma, P.G. Kazansky, J. Qiu, Phys. Rev. Lett. 91 (2003) 247405.
[35] R. Taylor, C. Hnatovsky, E. Simova, Laser Phot. Rev. 2 (1–2) (2008) 26.
[36] W. Yang, E. Bricchi, P.G. Kazansky, J. Bovatsek, A.Y. Arai, Opt. Express 14 (21) (2006) 10117.
[37] W. Yang, P.G. Kazansky, Y.P. Svirko, Nat. Photonics 2 (2008) 99.
[38] P.G. Kazansky, W. Yang, E. Bricchi, J. Bovatsek, A. Arai, Y. Shimotsuma, K. Miura, K. Hirao, Appl. Phys. Lett. 90 (2007) 151120.
[39] I. Miyamoto, A. Horn, J. Gottmann, D. Wortmann, F. Yoshino, JLMN – J. Laser Micro/Nanoeng. 2 (1) (2007) 57.
[40] W. Yang, P. Kazansky, Y. Shimotsuma, M. Sakakura, K. Miura, K. Hirao, Appl. Phys. Lett. 93 (2008) 171109.
[41] K.C. Vishnubhatla, S. Venugopal Rao, R.S.S. Kumar, S.N.B. Bhaktha, A. Chiappini, A. Chiasera, J. Laureyns, M. Ferrari, M. Mattarelli, M. Montagna, R. Osellame, R. Ramponi, G.C. Righini, S. Turrell, D. Narayana Rao, Proc. SPIE 6881 (2008) 688114.
[42] A. Zoubir, C. Lopez, M. Richardson, K. Richardson, Opt. Lett. 29 (2004) 1840.
[43] A. Zoubir, C. Rivero, R. Grodsky, K. Richardson, M. Richardson, T. Cardinal, M. Couzi, Phys. Rev. B. 73 (2006) 224117.
[44] G. Li, K.A. Winick, A.A. Said, M. Dugan, P. Bado, Opt. Lett. 31 (6) (2006) 739.
[45] J.W. Chan, T.R. Huster, S.H. Risbud, D.M. Krol, Appl. Phys. A76 (2003) 367.
[46] Y. Li, C. Xing, Y. Ma, J. Tian, J. Xu, Q. Sun, J. Opt. A: Pure Appl. Opt. 11 (2009) 045601.
[47] A. Zoubir, M. Richardson, L. Canioni, A. Brocas, L. Sarger, J. Opt. Soc. Am. B. 22 (10) (2005) 2138.
[48] Y. Bellouard, A. Said, M. Dugan, P. Bado, Opt. Express 12 (10) (2004) 2120.
[49] W.J. Reichman, D.M. Krol, L. Shah, F. Yoshino, A. Arai, S.M. Eaton, P.R. Herman, J. Appl. Phys. 99 (2006) 123112.
[50] J. Liu, Z. Zhang, Z. Lu, G. Xiao, F. Sun, S. Chang, C. Flueraru, Appl. Phys. B 86 (2007) 151.
[51] G.D. Marshall, M. Ams, M.J. Withford, Opt. Lett. 31 (18) (2006) 2690.
[52] J. Ihlemann, S. Müller, S. Puschmann, D. Schäfer, P.R. Herman, J. Li, M. Wei, Proc. SPIE 4941 (2003) 94.
[53] J. Song, X. Wang, X. Hu, Y. Dai, J. Qiu, Y. Cheng, Z. Xu, Appl. Phys. Lett. 92 (2008) 092904.
[54] T. Hashimoto, S. Juodkazis, H. Misawa, Appl. Phys. A 83 (2006) 337.
[55] D.-L. Wang, C.-D. Li, L. Luo, H. Yang, Q.-H. Gong, Chin. Phys. Lett. 18 (1) (2001) 65.
[56] S. Juodkazis, H. Misawa, T. Hashimoto, E.G. Gamaly, B. Luther-Davies, Appl. Phys. Lett. 88 (2006) 201909.
[57] C. Mendez, J.R. Ýazquez de aldana, G.A. Torchia, L. Roso, Appl. Phys. B 86 (2007) 343.
[58] W. Watanabe, T. Toma, K. Yamada, J. Nishii, Ken-ichi Hayashi, K. Itoh, Opt. Lett. 25 (22) (2000) 1669.
[59] E. Toratani, M. Kamata, M. Obara, Appl. Phys. Lett. 87 (2005) 171103.
[60] H. Sun, J. Song, C. Li, J. Xu, X. Wang, Y. Cheng, Z. Xu, J. Qiu, T. Jia, Appl. Phys. A 88 (2007) 285.
[61] A. Mermillod-Blondin, J. Bonse, A. Rosenfeld, I.V. Hertel, Yu.P. Meshcheryakov, N.M. Bulgakova, E. Audouard, R. Stoian, Appl. Phys. Lett. 94 (2009) 041911.
[62] F.L. Galeener, J. Non-Cryst. Solids 71 (1985) 373.
[63] R.A. Barrio, F.L. Galeener, E. Marinez, R.J. Elliot, Phys. Rev. B 48 (1993) 15672.
[64] F. Vega, J. Armengol, V. Diez-Blanco, J. Siegel, J. Solis, B. Barcones, A. Pérez-Rodríguez, P. Loza-Alvarez, Appl. Phys. Lett. 87 (2005) 021109.
[65] T. Hongo, K. Sugioka, H. Niino, Y. Cheng, M. Masuda, J. Miyamoto, H. Takai, K. Midorikawa, J. Appl. Phys. 97 (2005) 063517.
[66] Z. Wang, K. Sugioka, K. Midorikawa, Appl. Phys. A. 89 (2007) 955.
[67] Z. Wang, K. Sugioka, K. Midorikawa, Appl. Phys. A 93 (2008) 225.
[68] R. An, Y. Li, D. Liu, Y. Dou, F. Qi, H. Yang, Q. Gong, App. Phys. A 86 (2007) 343.
[69] Z.L. Li, D.K.Y. Low, M.K. Ho, G.C. Lim, K.J. Moh, J. Laser Appl. 18 (2006) 320.
[70] V.R. Bhardwaj, E. Simova, P.B. Corkum, D.M. Rayner, C. Hnatovsky, R.S. Taylor, B. Schreder, M. Kluge, J. Zimmer, J. Appl. Phys. 97 (2005) 083102.
[71] J. Stillman, J. Judy, H. Helvajian, Proc. SPIE 6882 (2008) 68820J.
[72] B. Fisette, F. Busque, J.-.Y. Degorce, M. Meunier, App. Phys. Lett. 88 (2006) 091104.
[73] A.A. Bettiol, S. Venugopal Rao, F. Watt, Appl. Phys. Lett. 88 (2006) 171106.
[74] A.A. Bettiol, E.J. Teo, C.N.B. Udalagama, S. Venugopal Rao, J.A. van Kan, P. Shao, F. Watt, Proc. SPIE 6186 (2006) 61860F.
[75] A.A. Bettiol, C.N.B. Udalagama, E.J. Teo, J.A. van Kan, F. Watt, Nucl. Instrum. Methods Phys. Res. B 260 (2007) 357.
[76] Q.-Z. Zhao, J.-R. Qiu, X.-W. Jiang, C.-J. Zhao, C.-S. Zhu, Opt. Express 12 (2004) 4035.